Solid state and solution structures of alkaline-earth complexes with lariat ethers containing aniline and benzimidazole pendants

Aurora Rodríguez-Rodríguez, Israel Carreira-Barral, Martín Regueiro-Figueroa, David Esteban-Gómez, Carlos Platas-Iglesias, Andrés de Blas*, Teresa Rodríguez-Blas†

Departamento de Química Fundamental, Facultad de Ciencias, Universidade da Coruña, Campus da Zapateira-Rúa da Fraga 10, 15008 A Coruña, Spain

Polyhedron, volume 31, issue 1, pages 402–412, 04 January 2012
Received 19 May 2011, accepted 25 September 2011, available online 12 October 2011

How to cite:
A. Rodríguez-Rodríguez, I. Carreira-Barral, M. Regueiro-Figueroa, D. Esteban-Gómez, C. Platas-Iglesias, A. De Blas, T. Rodríguez-Blas, Solid state and solution structures of alkaline-earth complexes with lariat ethers containing aniline and benzimidazole pendants, Polyhedron. 31 (2012) 402–412. https://doi.org/10.1016/j.poly.2011.09.027.

Abstract

Herein we report the synthesis and structural characterization of Mg(II), Ca(II), Sr(II) and Ba(II) complexes with bibracchial lariat ethers derived from 1,7-diaza-15-crown-5 and 1,7-diaza-12-crown-4 containing aniline or benzimidazole pendant arms. The solid state structures of most of them have been determined by using single crystal X-ray crystallography. A coordination number of seven was observed for the Mg(II) complexes in the solid state, while the Ca(II), Sr(II) and Ba(II) complexes are 8-, 9- and 11-coordinate, respectively. The Ca(II), Sr(II) and Ba(II) complexes show a *syn* conformation, with the two pendant arms of the ligand disposed on the same side of the macrocyclic mean plane. However, the Mg(II) complex with the largest ligand derived from 1,7-diaza-15-crown-5 containing benzimidazole pendants presents an *anti* conformation in the solid state. ^{1}H and ^{13}C NMR spectroscopy reveal that this conformation is maintained in acetonitrile solution.

Keywords: macrocyclic ligands; crystal structures; crown ethers; alkaline-earth complexes

1. **Introduction**

Crown and aza-crown ethers constitute an important class of macrocyclic multidentate receptors extensively used in metal ion separations [1,2]. Attachment of side arms with potential metal ion binding sites to a (aza)crown ether gives lariat ethers [3], which provide a three dimensional complexation that often results in enhanced cation binding affinity and selectivity in comparison to the parent macrocycle [4,5]. Due to their

* andres.blas@udc.es
† teresa.rodriguez.blas@udc.es

interesting recognition properties, crown and lariat ethers have found many applications in different areas that include: (i) separation and transport processes for the recovery or removal of metal ions [6]; (ii) preparation of ion-selective electrodes [7,8] and stationary phases in chromatographic techniques [9]; (iii) the design of chromogenic or fluorogenic chemosensors [10,11,12]; or (iv) their use as phase-transfer catalysts in organic reactions [13,14]. Furthermore, crown ethers have also considerable biochemical relevance as models of natural ionophores [15]. More recently it has been also suggested that crown ethers may find application as novel anticancer drugs [16].

The coordination chemistry of the group 2 cations is subject of continuous interest, mainly due to their importance in the human body. For instance, Ca(II) is a vital cation essential for formation of the bone structures of mammals [17], and acts as a second messenger in signal transduction and in the transmission of nerve impulses [18]. Mg(II) exerts a large variety of biological functions, ranging from structural roles by forming complexes with negatively charged groups (i.e. phosphates in nucleic acids), catalytic roles in enzyme activation or inhibition, and regulatory roles by modulating cell proliferation, cell cycle progression and differentiation [19]. Several evidences support the role of Sr(II) in anabolic activity in the skeletal system, although strontium is not yet considered as essential for humans [20]. Because of its similarity to calcium and its bone-seeking behavior, Sr(II) accumulates in bone, can displace calcium in hard tissue metabolic processes, and at high concentrations interferes with normal bone development [21,22].

In previous papers we have reported the coordinative properties towards Mg(II), Ca(II), Sr(II) and Ba(II) of the bibracchial lariat ethers **L**^{5} and **L**^{6} (Scheme 1), which contain a 1,10-diaza-18-crown-6 platform and aniline or benzimidazole pendant arms [23,24]. As a continuation of these works, herein we report an structural study both in the solid state and solution of alkaline-earth complexes with the related receptors **L**^{1}–**L**^{4} (Scheme 1). The aim of the present study is to investigate the effect of the size of the crown moiety on the coordinative properties of this family of closely related complexes.

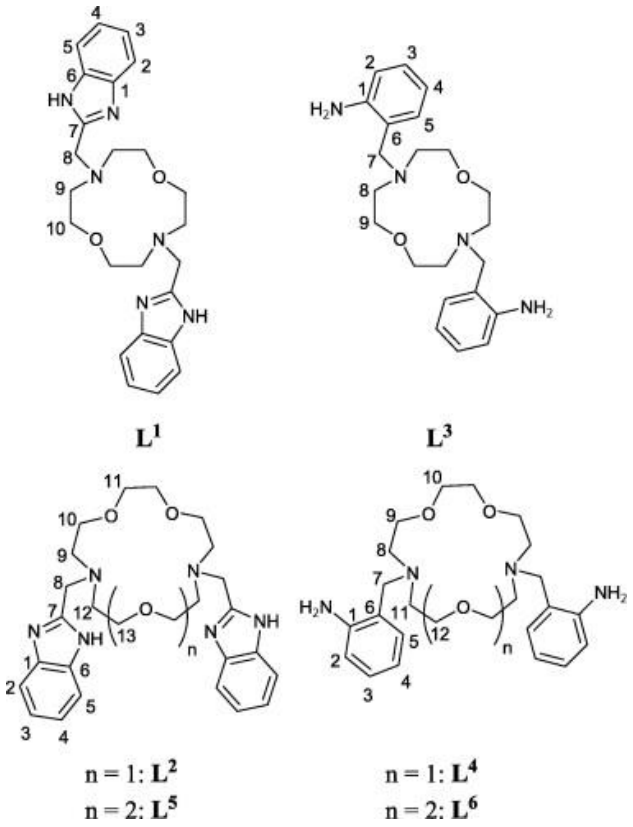

Scheme 1.

2. **Experimental**

2.1. Reagents

N,*N*′-bis(benzimidazol-2ylmethyl)-1,7-diaza-12-crown-4 (**L**^{1}) [25], *N*,*N*′-bis(benzimidazol-2ylmethyl)-1,7-diaza-15-crown-5 (**L**^{2}) [25], *N*,*N*′-bis(2-aminobenzyl)-1,7-diaza-12-crown-4 (**L**^{3}) [26] and *N*,*N*′-bis(2-aminobenzyl)-1,7-diaza-15-crown-5 (**L**^{4}) [27], were prepared according to the literature methods. All other chemicals were purchased from commercial sources and used without further purification. Solvents were of reagent grade purified by the usual methods. Single crystals of **L**^{3} suitable for X-ray diffraction analysis were grown by slow evaporation of a solution of the ligand in ethanol at room temperature. *Caution!* Although we have experienced no difficulties with the perchlorate salts, these should be regarded as potentially explosive and handled with care [28].

2.2. Synthesis

2.2.1. *[Mg(**L**^{1})](ClO$_4$)$_2$·0.5EtOH·0.5H$_2$O (**1a**)*

A solution of $Mg(ClO_4)_2$ (0.057 g, 0.255 mmol) in absolute ethanol (5 mL) was added to a stirred solution of **L**^{1} (0.100 g, 0.231 mmol) in the same solvent (20 mL). The resulting mixture was refluxed for 24 h. The white precipitate formed was isolated by filtration and dried under vacuum. Yield: 0.137 g (86%). *Anal*. Calc. for $C_{25}H_{34}Cl_2MgN_6O_{11}$: C, 43.5; H, 5.0; N, 12.2. Found: C, 43.5; H, 4.8; N, 12.0%. FAB-MS: *m/z* (%BPI): 557(18) [Mg(**L**^{1})(ClO$_4$)]$^+$, 457(34) [Mg(**L**^{1}-H)]$^+$, 229(7) [Mg(**L**^{1})]$^{2+}$. IR (cm^{-1}): 1619 ($\nu_{C=N}$), 1541 ($\nu_{C=C}$), 1079 (ν_{Cl-O}), 622 (δ_{Cl-O}). Λ_M (cm^2 Ω^{-1} mol^{-1}): 277. Colorless single crystals of formula [Mg(**L**^{1})(H$_2$O)$_{0.18}$(MeOH)$_{0.82}$](ClO$_4$)$_2$·0.18(MeOH) (**1b**) suitable for single crystal X-ray diffraction analysis were obtained by slow diffusion of diethyl ether into a solution of the complex in methanol.

2.2.2. *[Ca(**L**^{1})](ClO$_4$)$_2$·EtOH·H$_2$O (**2a**)*

A solution of $Ca(ClO_4)_2·4H_2O$ (0.079 g, 0.255 mmol) in absolute ethanol (5 mL) was added to a stirred solution of **L**^{1} (0.100 g, 0.231 mmol) in the same solvent (20 mL). The resulting mixture was refluxed for 24 h. The solution was filtered while hot and the filtrate allowed evaporating at room temperature to give a white solid that was isolated by filtration and dried under vacuum. Yield: 0.036 g (21%). *Anal*. Calc. for $C_{26}H_{38}CaCl_2N_6O_{12}$: C, 42.3; H, 5.2; N, 11.4. Found: C, 42.2; H, 5.3; N, 11.2%. FAB-MS: *m/z* (%BPI): 573(64) [Ca(**L**^{1})(ClO$_4$)]$^+$, 473(39) [Ca(**L**^{1}-H)]$^+$, 237(10) [Ca(**L**^{1})]$^{2+}$. IR (cm^{-1}): 1639 ($\nu_{C=N}$), 1541 ($\nu_{C=C}$), 1076 (ν_{Cl-O}), 622 (δ_{Cl-O}). Λ_M (cm^2 Ω^{-1} mol^{-1}): 301. Colorless single crystals of which [Ca(**L**^{1})(MeOH)$_2$](ClO$_4$)$_2$·(**2b**) suitable for single crystal X-ray diffraction analysis were obtained by slow diffusion of diethyl ether into a solution of the complex in methanol.

2.2.3. *[Sr(**L**^{1})](ClO$_4$)$_2$·2H$_2$O (**3a**)*

The preparation of this compound, which was isolated as a pale brown powder, followed the same procedure described for **2a** by using a solution of $Sr(ClO_4)_2·H_2O$ (0.073 g, 0.255 mmol). Yield: 0.148 g (84%). *Anal*. Calc. for $C_{24}H_{34}Cl_2N_6O_{12}Sr$: C, 38.1; H, 4.5; N, 11.1. Found: C, 38.1; H, 4.4; N, 11.0%. FAB-MS: *m/z* (%BPI): 621(100) [Sr(**L**^{1})(ClO$_4$)]$^+$, 521(29) [Sr(**L**^{1}-H)]$^+$, 261(6) [Sr(**L**^{1})]$^{2+}$. IR (cm^{-1}): 1622 ($\nu_{C=N}$), 1536 ($\nu_{C=C}$), 1085 (ν_{Cl-O}), 619 (δ_{Cl-O}). Λ_M (cm^2 Ω^{-1} mol^{-1}): 290. Colorless single crystals of formula [Sr(**L**^{1})(MeOH)(ClO$_4$)](ClO$_4$)·MeOH·Et$_2$O (**3b**) suitable for single crystal X-ray diffraction analysis were obtained by slow diffusion of diethyl ether into a solution of the complex in methanol.

2.2.4. *[Ba(**L**^{1})](ClO$_4$)$_2$·0.5H$_2$O (**4a**)*

The preparation of this compound, which was isolated as a white powder, followed the same procedure described for **1a** by using a solution of $Ba(ClO_4)_2·3H_2O$ (0.100 g, 0.255 mmol). Yield: 0.143 g (79%). *Anal*. Calc. for $C_{24}H_{31}BaCl_2N_6O_{10.5}$: C, 37.0; H, 4.0; N, 10.8. Found: C, 37.3; H, 3.8; N, 10.8%. FAB-

MS: *m/z* (%BPI): 671(34) [Ba(**L**^{1})(ClO_4)]$^+$, 571(14) [Ba(**L**^{1}-H)]$^+$. IR (cm^{-1}): 1623 ($\nu_{C=N}$), 1538 ($\nu_{C=C}$), 1086 (ν_{Cl-O}), 617 (δ_{Cl-O}). Λ_M ($cm^2\ \Omega^{-1}\ mol^{-1}$): 265. Colorless single crystals of formula [Ba(**L**^{1})(MeOH)(ClO_4)$_2$] (**4b**) suitable for single crystal X-ray diffraction analysis were obtained by slow diffusion of diethyl ether into a solution of the complex in methanol.

2.2.5. *[Mg(**L**^{2})](ClO_4)$_2$·0.5EtOH·0.5H_2O (**5a**)*

The preparation of this compound, which was isolated as a white powder, followed the same procedure described for **1a** by using $Mg(ClO_4)_2$ (0.051 g, 0.230 mmol) and **L**^{2} (0.100 g, 0.209 mmol). Yield: 0.129 g (84%). *Anal.* Calc. for $C_{27}H_{38}Cl_2MgN_6O_{12}$: C, 44.2; H, 5.2; N, 11.5. Found: C, 44.2; H, 4.8; N, 11.7%. FAB-MS: *m/z* (%BPI): 601(46) [Mg(**L**^{2})(ClO_4)]$^+$, 501(100) [Mg(**L**^{2}-H)]$^+$, 251(16) [Mg(**L**^{2})]$^{2+}$. IR (cm^{-1}): 1622 ($\nu_{C=N}$), 1541 ($\nu_{C=C}$), 1094 (ν_{Cl-O}), 618 (δ_{Cl-O}). Λ_M ($cm^2\ \Omega^{-1}\ mol^{-1}$): 307. Colorless single crystals of formula [Mg(**L**^{2})](ClO_4)$_2$·MeOH (**5b**) suitable for single crystal X-ray diffraction analysis were obtained by slow diffusion of diethyl ether into a solution of the complex in methanol.

2.2.6. *[Ca(**L**^{2})](ClO_4)$_2$·0.5EtOH·0.5H_2O (**6a**)*

The preparation of this compound, which was isolated as a white powder, followed the same procedure described for **1a** by using $Ca(ClO_4)_2$·4H_2O (0.072 g, 0.230 mmol) and **L**^{2} (0.101 g, 0.210 mmol). Yield: 0.114 g (72%). *Anal.* Calc. for $C_{27}H_{38}CaCl_2N_6O_{12}$: C, 43.3; H, 5.1; N, 11.2. Found: C, 43.3; H, 4.6; N, 11.6%. FAB-MS: *m/z* (%BPI): 617(100) [Ca(**L**^{2})(ClO_4)]$^+$, 517(81) [Ca(**L**^{2}-H)]$^+$, 259(11) [Ca(**L**^{2})]$^{2+}$. IR (cm^{-1}): 1623 ($\nu_{C=N}$), 1538 ($\nu_{C=C}$), 1086 (ν_{Cl-O}), 618 (δ_{Cl-O}). Λ_M ($cm^2\ \Omega^{-1}\ mol^{-1}$): 282. Colorless single crystals of formula [Ca(**L**^{2})(ClO_4)](ClO_4) (**6b**) suitable for single crystal X-ray diffraction analysis were obtained by slow diffusion of diethyl ether into a solution of the complex in acetonitrile.

2.2.7. *[Sr(**L**^{2})](ClO_4)$_2$·H_2O (**7a**)*

The preparation of this compound, which was isolated as a white powder, followed the same procedure described for **1a** by using $Sr(ClO_4)_2$·H_2O (0.066 g, 0.231 mmol) and **L**^{2} (0.100 g, 0.209 mmol). Yield: 0.148 g (90%). *Anal.* Calc. for $C_{26}H_{36}Cl_2N_6O_{12}Sr$: C, 39.9; H, 4.6; N, 10.7. Found: C, 39.9; H, 4.5; N, 10.7%. FAB-MS: *m/z* (%BPI): 665(83) [Sr(**L**^{2})(ClO_4)]$^+$, 565(46) [Sr(**L**^{2}-H)]$^+$, 283(9) [Sr(**L**^{2})]$^{2+}$. IR (cm^{-1}): 1623 ($\nu_{C=N}$), 1536 ($\nu_{C=C}$), 1082 (ν_{Cl-O}), 619 (δ_{Cl-O}). Λ_M ($cm^2\ \Omega^{-1}\ mol^{-1}$): 254. Colorless single crystals of formula [Sr(**L**^{2})(ClO_4)](ClO_4)·CH_3CN·EtOH (**7b**) suitable for single crystal X-ray diffraction analysis were obtained by slow diffusion of diethyl ether into a solution of the complex in acetonitrile.

2.2.8. *[Ba(**L**^{2})(ClO_4)$_2$] (**8**)*

The preparation of this compound, which was isolated as a white powder, followed the same procedure described for **1a** by using $Ba(ClO_4)_2$·3H_2O (0.090 g, 0.231 mmol) and **L**^{2} (0.100 g, 0.209 mmol). Yield: 0.132 g (77%). *Anal.* Calc. for $C_{26}H_{34}BaCl_2N_6O_{11}$: C, 38.3; H, 4.2; N, 10.3. Found: C, 38.2; H, 4.2; N, 10.3%. FAB-MS: *m/z* (%BPI): 715(19) [Ba(**L**^{2})(ClO_4)]$^+$, 615(13) [Ba(**L**^{2}-H)]$^+$, 307(38) [Ba(**L**^{2})]$^{2+}$. IR (cm^{-1}): 1622 ($\nu_{C=N}$), 1535 ($\nu_{C=C}$), 1091 (ν_{Cl-O}), 616 (δ_{Cl-O}). Λ_M ($cm^2\ \Omega^{-1}\ mol^{-1}$): 268. Single crystals of formula **8** suitable for single crystal X-ray diffraction analysis were obtained by slow evaporation of the mother liquor.

2.2.9. *[Ca(**L**^{3})](ClO_4)$_2$·2H_2O (**9a**)*

A solution of $Ca(ClO_4)_2$·4H_2O (0.121 g, 0.390 mmol) in absolute ethanol (10 mL) was added to a solution of **L**^{3} (0.150 g, 0.390 mmol) in the same solvent (10 mL). The resulting mixture was refluxed for 24 h. The white precipitate formed was isolated by filtration, washed with diethyl ether and air-dried. Yield: 0.182 g (75%). *Anal.* Calc. for $C_{22}H_{36}CaCl_2N_4O_{12}$: C, 40.1; H, 5.5; N, 8.5. Found: C, 40.0; H, 5.5; N, 8.4%. FAB-MS: *m/z* (%BPI): 523(100) [Ca(**L**^{3})(ClO_4)]$^+$, 423(9) [Ca(**L**^{3}-H)]$^+$. IR (cm^{-1}): 3355, 3295 (ν_{N-H}), 1619 (δ_{N-H}),

1070 (ν_{Cl-O}), 622 (δ_{Cl-O}). Λ_M ($cm^2\ \Omega^{-1}\ mol^{-1}$): 255. Single crystals of empirical formula $C_{22.75}H_{37.25}CaCl_2N_4O_{12.20}$ (**9b**) suitable for single crystal X-ray diffraction analysis were obtained by slow evaporation of the mother liquor.

2.2.10. *[Sr(**L**^{3})](ClO$_4$)$_2$ (**10**)*

A solution of $Sr(ClO_4)_2 \cdot 4H_2O$ (0.091 g, 0.260 mmol) in absolute ethanol (10 mL) was added to a solution of **L**^{3} (0.100 g, 0.260 mmol) in the same solvent (10 mL). The resulting mixture was refluxed for 24 h. The solvent was evaporated, and absolute ethanol (~3 mL) were added. Yield: 0.057 g (33%). *Anal*. Calc. for $C_{26}H_{32}Cl_2N_4O_{10}Sr$: C, 39.4; H, 4.8; N, 8.35. Found: C, 39.2; H, 5.2; N, 7.8%. FAB-MS: *m*/*z* (%BPI): 571(48) [Sr(**L**^{3})(ClO$_4$)]$^+$, 471(3) [Sr(**L**^{3}-H)]$^+$. IR (cm^{-1}): 3384, 3318 (ν_{N-H}), 1613 (δ_{N-H}), 1066 (ν_{Cl-O}), 621 (δ_{Cl-O}). Λ_M ($cm^2\ \Omega^{-1}\ mol^{-1}$): 255.

2.2.11. *[Ba(**L**^{3})](ClO$_4$)$_2$·2H$_2$O (**11**)*

A solution of $Ba(ClO_4)_2 \cdot 3H_2O$ (0.112 g, 0.260 mmol) in absolute ethanol (10 mL) was added to a solution of **L**^{3} (0.100 g, 0.260 mmol) in the same solvent (10 mL). The resulting mixture was refluxed for 24 h. The white precipitate formed was isolated by filtration, washed with diethyl ether and air-dried. Yield: 0.118 g (60%). *Anal*. Calc. for $C_{22}H_{36}BaCl_2N_4O_{12}$: C, 34.9; H, 4.8; N, 7.4. Found: C, 34.8; H, 5.0; N, 7.3%. FAB-MS: *m*/*z* (%BPI): 621(84) [Ba(**L**^{3})(ClO$_4$)]$^+$, 521(3) [Ba(**L**^{3}-H)]$^+$. IR (cm^{-1}): 3391, 3322 (ν_{N-H}), 1610 (δ_{N-H}), 1065 (ν_{Cl-O}), 622 (δ_{Cl-O}). Λ_M ($cm^2\ \Omega^{-1}\ mol^{-1}$): 294.

2.2.12. *[Ca(**L**^{4})](ClO$_4$)$_2$ (**12**)*

A solution of $Ca(ClO_4)_2 \cdot 4H_2O$ (0.109 g, 0.350 mmol) in absolute ethanol (10 mL) was added to a solution of **L**^{4} (0.150 g, 0.350 mmol) in the same solvent (10 mL). The resulting mixture was refluxed for 24 h. The white precipitate formed was isolated by filtration, washed with diethyl ether and air-dried. Yield: 0.179 g (77%). *Anal*. Calc. for $C_{24}H_{36}CaCl_2N_4O_{11}$: C, 43.2; H, 5.4; N, 8.4. Found: C, 43.1; H, 5.7; N, 8.7%. FAB-MS: *m*/*z* (%BPI): 567(64) [Ca(**L**^{4})(ClO$_4$)]$^+$, 467(8) [Ca(**L**^{4}-H)]$^+$. IR (cm^{-1}): 3343, 3286 (ν_{N-H}), 1615 (δ_{N-H}), 1054 (ν_{Cl-O}), 620 (δ_{Cl-O}). Λ_M ($cm^2\ \Omega^{-1}\ mol^{-1}$): 295.

2.2.13. *[Sr(**L**^{4})(ClO$_4$)](ClO$_4$) (**13**)*

The preparation of this compound, which was isolated as a white powder, followed the same procedure described for **12** by using a solution of $Sr(ClO_4)_2 \cdot 4H_2O$ (0.123 g, 0.350 mmol). Yield: 0.175 g (70%). *Anal*. Calc. for $C_{24}H_{36}Cl_2N_4O_{11}Sr$: C, 40.3; H, 5.1; N, 7.8. Found: C, 40.5; H, 5.2; N, 8.1%. FAB-MS: *m*/*z* (%BPI): 615(17) [Sr(**L**^{4})(ClO$_4$)]$^+$, 515(4) [Sr(**L**^{4}-H)]$^+$. IR (cm^{-1}): 3367, 3299 (ν_{N-H}), 1616 (δ_{N-H}), 1062 (ν_{Cl-O}), 621 (δ_{Cl-O}). Λ_M ($cm^2\ \Omega^{-1}\ mol^{-1}$): 295. Colorless single crystals of **13** suitable for single crystal X-ray diffraction analysis were obtained by slow diffusion of diethyl ether into a solution of the complex in methanol.

2.3. Measurements

Elemental analyses were carried out on a Carlo Erba 1108 elemental analyzer. FAB mass spectra were recorded on a Fisons Quatro mass spectrometer with a Cs ion gun using 3-nitrobenzyl alcohol as matrix. ^{1}H and ^{13}C NMR spectra were run on a Bruker Advance 500 using acetonitrile-d_3 as solvent. IR spectra were recorded using a Bruker Vector 22 spectrophotometer equipped with a Golden Gate Attenuated Total Reflectance (ATR) accessory (Specac). Conductivity measurements were carried out with a Crison Micro CM 2201 conductivimeter using ca. 10^{-3} M solutions of the complexes in acetonitrile.

2.4. X-ray crystallography

Three-dimensional X-ray data were collected on a Bruker-Nonius X8 Apex-Kappa CCD diffractometer by the omega and phi scan method. Reflections were measured from a hemisphere of data collected of frames each covering 0.5° in omega. The reflections measured were corrected for Lorentz and polarization effects and for absorption by semi-empirical methods based on symmetry-equivalent and repeated reflections [29], except in the case of **L³** for which no absorption correction was performed. The solution, refinement and analysis of the single crystal X-ray diffraction data was performed with WinGX suite for small molecule single-crystal crystallography [30]. The structures were solved either by Patterson methods with DIRDIF2008 [31] (**2b**, **3b**, **5b**, **7b**, **8**, and **9b**) or SIR92 (**13**) [32], by direct methods with shelxs-97 [33] (**1b** and **6b**), or by using the charge flipping in arbitrary dimensions algorithm with Superflip (**L³** and **4b**) [34]. All the structures were refined by full-matrix least-square methods on F^2 with shelxl97 [33]. Most of hydrogen atoms were included in calculated positions and refined by using a riding mode. The exceptions were the following: (a) the protons of the aniline group in **L³** and **13**, which were refined freely; (b) the hydrogen atom of the coordinated methanol in **1a**, which was located in a difference electron-density map and refined freely, and the hydrogen atoms of the coordinated water molecule which were located with CALC-OH [35] and all positional parameters fixed; (c) the hydrogen atom bonded to the oxygen atom of the methanol molecule coordinated to the metal ion in **2b**, which was located in a difference electron-density map and refined freely; (d) the hydrogen atoms of OH groups of both methanol molecules in **3b** (the coordinated and the not coordinated one), which were located in a difference electron-density map and refined freely; (e) the same treatment was used for the OH hydrogen atom of the coordinated methanol molecule in **4b**, while for **5b** the hydrogen atoms of OH groups of both methanol molecules were located in a difference electron-density map and all positional parameters fixed. In the case of **9b**, it was not possible to find water hydrogen atoms bonded to O(1W), while other water hydrogen atoms as well as the alcoholic hydrogen atom of the coordinated ethanol molecule were located in a difference electron-density map and all positional parameters fixed. On the other hand, three of the crystals (**1b**, **5b**, and **9b**) show positional and/or substitutional disorder that was solved. Compound **1b** contains two disordered non-coordinated perchlorate groups with occupation factors for the main positions centered in Cl(1A) and Cl(2A) of 0.80(1) and 0.830(4), respectively. The crown moiety also shows positional disorder with occupation factors of 0.515(3) for positions labeled with A. Finally, **1a** shows a substitutional disorder in one of the coordination positions of Mg that is occupied alternatively by a water molecule (0.181(4)), or a methanol molecule (0.819(4)). When a water molecule is bonded to the Mg ion, a non-coordinated methanol molecule (occupation factor 0.181(4)) was also included in the model. Compound **5b** shows positional disorder for two perchlorate groups centered in Cl(2) and Cl(3) and a non-coordinated methanol molecule with occupation factors for the main positions of 0.852(7), 0.64(1) and 0.77(1), respectively. Finally, compound **9b** shows positional disorder for the perchlorate group centered in Cl(2) (occupation factor for the main position 0.680(4)) and substitutional disorder for one of the coordinated molecules, the coordination position being occupied alternatively by an ethanol molecule (0.34(2) or a water molecule (0.66(2)). In the latter case, another non-bonded water molecule (occupation factor 0.20(2)) was found, but its hydrogen atoms could not be reliably located due to the very small electron density. The position of H(41) bonded to O(4W) is not reliable either. Refinement converged with allowance for thermal anisotropy of all non-hydrogen atoms in every case. Crystal data and details on data collection and refinement are summarized in Table 1, Table 2, Table 3.

3. **Results and discussion**

3.1. Synthesis and characterization

Compounds of formula M(**L¹**)$(ClO_4)_2 \cdot x$EtOH$\cdot y H_2O$ (M = Mg, Ca, Sr or Ba), M(**L²**)$(ClO_4)_2 \cdot x$EtOH$\cdot y H_2O$ (M = Mg, Ca, Sr or Ba), M(**L³**)$(ClO_4)_2 \cdot x H_2O$ (M = Ca, Sr or Ba) and M(**L⁴**)$(ClO_4)_2$ (M = Ca or Sr) were

prepared by reaction of the corresponding ligand with the respective metal perchlorate in ethanol under the conditions described in Section 2. Attempts to isolate the corresponding Mg(II) complexes with **L³** and **L⁴** by using similar synthetic conditions were unsuccessful. The [Ba(**L⁴**)(ClO_4)](ClO_4) complex was previously prepared by us and its solid state and solution structure reported [36].

Table 1. Crystal data and structure refinement for **1b**, **2b**, **3b** and **4b**.

	1b	**2b**	**3b**	**4b**
Empirical formula	$C_{25}H_{34}Cl_2MgN_6O_{11}$	$C_{26}H_{38}CaCl_2N_6O_{12}$	$C_{30}H_{48}Cl_2N_6O_{13}Sr$	$C_{25}H_{34}BaCl_2N_6O_{11}$
Molecular weight	694.04	737.60	859.26	802.82
T (K)	100.0(2)	100.0(2)	100.0(2)	100.0(2)
Wavelength (Å)	0.71073	0.71073	0.71073	0.71073
Crystal system	monoclinic	monoclinic	monoclinic	monoclinic
Space group	$P2_1/n$	$C2/c$	$P2_1/c$	$C2/c$
a (Å)	10.7150(3)	19.2013(5)	9.0647(4)	26.4553(6)
b (Å)	17.8898(5)	10.7161(4)	12.7259(5)	16.8499(5)
c (Å)	15.6339(5)	16.8772(5)	32.6147(12)	18.1873(8)
α (°)	90	90	90	90
β (°)	90.970(3)	110.861(2)	97.715(2)	131.9040(10)
γ (°)	90	90	90	90
V (Å³)	2996.4(2)	3245.1(2)	3728.3(3)	6034.0(4)
F(0 0 0)	1449	1544	1784	3232
Z	4	4	4	8
D_{calc} (g cm^{-3})	1.538	1.510	1.531	1.767
Absorption coefficient μ (mm^{-1})	0.309	0.429	1.660	1.563
θ Range for data collection (°)	2.62–28.38	2.58–28.43	2.44–28.42	2.24–28.44
R_{int}	0.0503	0.0247	0.0988	0.0219
Reflections measured	44 790	16 188	69 502	31 210
Reflections observed	5411	3594	6608	6935
Goodness-of-fit (GOF) on F^2	1.027	1.062	1.011	1.063
R_1[a]	0.0404	0.0328	0.0433	0.0197
wR_2 (all data)[b]	0.0979	0.0911	0.0948	0.0515
Largest differences in peak and hole (e Å^{-3})	0.377 and −0.351	0.679 and −0.562	0.429 and −0.487	0.610 and −0.503

[a] $R_1 = \Sigma|F_o - F_c|/\Sigma F_o$. [b] $wR_2 = \{\Sigma[w(F_o^2 - F_c^2)^2]/\Sigma[w(F_o^4)]\}^{1/2}$.

The FAB-MS show intense peaks due to the [M(**L**^{n})(ClO_4)]$^+$ and [M(**L**^{n}-H)]$^+$ (n = 1–4) entities, which confirms the formation of the expected complexes. The IR spectra of **L³** and **L⁴** complexes display bands at ca. 3370 and 3300 cm^{-1} corresponding respectively to the $\nu_{as}(NH_2)$ and $\nu_s(NH_2)$ stretching modes of the coordinated amine groups, whereas the IR spectra of **L¹** and **L²** complexes show a band at ca. 1538 cm^{-1} due to the ν(C=C) stretching frequency of the benzimidazole groups [25]. This band is shifted by ~15 cm^{-1} to higher wavenumbers with respect to its position in the spectrum of the free ligand, in line with the coordination of the pendant arms to the corresponding metal ion. In all cases, bands corresponding to the ν_{as}(ClO) stretching and δ_{as}(OClO) bending modes of the perchlorate groups are observed, as uninformative broad bands, at ca. 1090–1070 and ca. 620 cm^{-1}, respectively [36,37]. The molar conductivity

values, as measured in ~10^{-3} M acetonitrile solutions of the complexes, fall in the range generally accepted for 2:1 electrolytes in this solvent (220–300 $cm^2\ \Omega^{-1}\ mol^{-1}$), suggesting that the perchlorate anions are not coordinated to the metal ion in solution [38].

Table 2. Crystal data and structure refinement for **5b**, **6b**, **7b** and **8**.

	5b	**6b**	**7b**	**8**
Empirical formula	$C_{27}H_{38}Cl_2MgN_6O_{12}$	$C_{26}H_{34}CaCl_2N_6O_{11}$	$C_{32}H_{47}Cl_2N_7O_{12}Sr$	$C_{26}H_{34}BaCl_2N_6O_{11}$
Molecular weight	733.84	717.57	880.29	814.83
T (K)	100(2)	100.0(2)	100.0(1)	100.0(2)
Wavelength (Å)	0.71073	0.71073	0.71073	0.71073
Crystal system	triclinic	monoclinic	monoclinic	monoclinic
Space group	$P\bar{1}$	$P2_1/c$	$P2_1/n$	$P2_1/c$
a (Å)	11.5169(7)	9.9276(5)	9.578(2)	9.0418(3)
b (Å)	12.2984(8)	21.6895(10)	14.418(2)	10.3455(3)
c (Å)	25.2086(15)	14.9410(7)	28.091(5)	33.7587(11)
α (°)	91.809(4)	90	90	90
β (°)	91.637(4)	108.539(3)	94.51(1)	96.436(2)
γ (°)	114.709(3)	90	90	90
V ($Å^3$)	3238.6(3)	3050.2(3)	3867(1)	3137.95(17)
F(0 0 0)	1536	1496	1824	1640
Z	4	4	4	4
D_{calc} (g cm^{-3})	1.505	1.563	1.512	1.725
Absorption coefficient μ (mm^{-1})	0.292	0.451	1.601	1.504
θ Range for data collection (°)	1.95–24.71	2.38–28.41	2.83–28.47	2.06–28.33
R_{int}	0.0597	0.0726	0.1386	0.0506
Reflections measured	33 619	32 015	39 275	31 203
Reflections observed	7512	5094	5445	6030
Goodness-of-fit (GOF) on F^2	1.061	1.010	0.993	1.030
R_1[a]	0.0761	0.0480	0.0573	0.0363
wR_2 (all data)[b]	0.2062	0.1123	0.132	0.0784
Largest differences in peak and hole (e $Å^{-3}$)	1.685 and −0.844	0.428 and −0.553	0.739 and −0.761	0.484 and −0.574

[a] $R_1 = \Sigma|F_o - F_c|/\Sigma F_o$. [b] $wR_2 = \{\Sigma[w(|F_o^2 - F_c^2|)^2]/\Sigma[w(F_o^4)]\}^{1/2}$.

3.2. NMR spectroscopy

The ^1H and ^{13}C NMR spectra of the Mg(II), Ca(II), Sr(II) and Ba(II) complexes of ligands **L¹** to **L⁴** were recorded in CD_3CN solution, and assigned with the aid of HSQC and HMBC 2D heteronuclear experiments, as well as standard 2D homonuclear COSY spectra (Table 4, Table 5). The ^1H NMR spectra of the complexes of **L¹** and **L²** (Fig. 1) show different signals for the axial and equatorial protons of the macrocyclic fragment. This indicates that the interconversion between the δ and λ conformations [39] of the five-membered chelate rings formed upon coordination of the crown moiety is slow in the NMR time-scale, pointing to a relatively rigid structure of the crown moiety in solution. This is compatible with hexadentate binding of **L¹** and heptadentate binding of **L²** to all metal ions, in line with the X-ray structures described below. The specific CH_2 proton assignments of the axial and equatorial protons of the macrocyclic moieties were not

possible on the basis of the 2D NMR spectra. However, it is known from previous ^{1}H NMR studies that the ring axial protons experience strong coupling with the geminal protons and the vicinal axial protons, while the equatorial protons provide strong coupling with the geminal protons only [40]. Indeed, the $^{3}J_{H–H}$ coupling constants characterizing the coupling between vicinal pairs of protons (axial–axial, axial–equatorial and equatorial–equatorial) follow the *Karplus* equation ($^{3}J_{H–H}$ = 7-cos ϕ + 5cos 2ϕ, where ϕ represents the H–C–C–H dihedral angle) [41,42]. According to our X-ray structures (see below), the ϕ values involving axial-axial vicinal protons are close to 180° (172–179°), while the dihedral angles defined by axial–equatorial and equatorial–equatorial vicinal protons fall within the range 52–66°. Thus, the specific assignment of the axial and equatorial protons could be achieved in some cases by observing the coupling pattern of the proton signals. For instance, the signal due to protons H9 at 2.68 ppm in [Sr(**L**^{2})]$^{2+}$ (Fig. 1), was assigned to equatorial protons, as the spin coupling pattern is dominated by a $^{2}J_{H-H}$ of 12–13 Hz, the $^{3}J_{H-H}$ values being substantially smaller (<4 Hz). In other cases the assignments of the equatorial and axial protons could be achieved by observing the cross-peaks in the COSY spectra, as axial protons are expected to give two strong cross-peaks (geminal and axial–axial), whereas equatorial protons should show one strong (geminal) and two weak (equatorial–equatorial and equatorial–axial) cross-peaks.

Table 3. Crystal data and structure refinement for **L**^{3}, **9b** and **13**.

	L^{3}	**9b**	**13**
Empirical formula	$C_{22}H_{32}N_4O_2$	$C_{22.75}H_{37.25}CaCl_2N_4O_{12.20}$	$C_{24}H_{36}Cl_2N_4O_{11}Sr$
Formula weight	384.52	673.8	715.09
T (K)	100.0(2)	100.0(2)	100(2)
Wavelength (Å)	0.71073	0.71073	0.71073
Crystal system	monoclinic	monoclinic	triclinic
Space group	$P2_1/c$	$P2_1/n$	$P\bar{1}$
a (Å)	7.261(3)	9.6070(6)	8.713(1)
b (Å)	18.840(9)	18.651(1)	10.775(1)
c (Å)	7.529(4)	16.508(1)	16.139(2)
α (°)	90	90	91.381(7)
β (°)	101.738(9)	99.535(4)	105.371(6)
γ (°)	90	90	101.266(7)
V (Å^3)	1008.4(8)	2916.9(3)	1428.2(3)
F(0 0 0)	416	1415	736
Z	2	4	2
D_{calc} (g cm^{-3})	1.266	1.534	1.663
Absorption coefficient μ (mm^{-1})	0.083	0.467	2.141
θ Range for data collection (°)	2.87–28.36	2.73–25.14	2.42–28.32
R_{int}	0.0905	0.0775	0.0428
Reflections measured	13 216	20 707	18 785
Reflections observed	2251	3296	5722
Goodness-of-fit (GOF) on F^2	1.066	1.020	1.032
R_1[a]	0.0424	0.0634	0.0336
wR_2 (all data)[b]	0.1118	0.1839	0.0739
Largest differences in peak and hole (e Å^{-3})	0.354 and −0.301	1.095 and −0.672	0.463 and −0.435

[a] $R_1 = \Sigma|F_o - F_c|/\Sigma|F_o|$. [b] $wR_2 = \{\Sigma[w(|F_o^2 - F_c^2|)^2]|/\Sigma[w(F_o^4)]\}^{1/2}$.

Table 4. ^{1}H and ^{13}C NMR spectral data [ppm with respect to TMS] in CD_3CN (298 K) of complexes with $\mathbf{L^1}$ and $\mathbf{L^2}$. See Scheme 1 for labeling.

	Mg[a]	Ca[b]	Sr[c]	Ba		Mg	Ca	Sr	Ba
$[M(\mathbf{L^1})]^{2+}$									
H2	7.58	7.58	7.55	7.55	C1	135.3	134.7	134.6	134.4
H3	7.19	7.30	7.25	7.30	C2	113.0	112.8	112.6	112.5
H4	6.80	7.22	7.28	7.30	C3	124.7	124.3	124.1	124.2
H5	6.80	7.67	7.86	7.92	C4	123.4	123.6	123.3	123.4
H8	4.29	4.14	4.14	4.09	C5	119.8	119.6	120.4	120.3
H9ax	3.02	2.76	2.73	2.71	C6	140.4	142.6	142.9	143.2
H9eq	3.17	3.00	2.92	2.87	C7	155.7	154.6	154.5	154.1
H10ax	3.81	3.87	3.80	3.78	C8	54.6	53.3	54.4	54.7
H10eq	3.70	3.94	3.80	3.84	C9	53.7	52.6	52.9	52.8
NH	11.28	11.08	11.08	10.91	C10	68.2	67.4	67.6	68.0
	Mg[d]	Ca[e]	Sr[f]	Ba[g]		Mg	Ca	Sr	Ba
$[M(\mathbf{L^2})]^{2+}$									
H2	7.80	7.53	7.53	7.56	C1	140.5	134.6	134.5	134.5
H3	7.39	7.18	7.21	7.29	C2	118.8	112.8	112.6	112.7
H4	7.39	6.94	7.06	7.29	C3	125.1	124.5	124.2	124.3
H5	7.67	6.84	7.36	7.82	C4	124.6	123.6	123.3	123.6
H8a	4.04	4.16	3.98	3.75	C5	113.4	119.0	119.5	119.5
H8b	4.55	4.24	4.17	4.30	C6	135.6	142.2	142.7	143.0
H9ax	2.71	3.01	3.06	3.01	C7	156.4	155.2	154.6	154.2
H9eq	3.06	2.98	2.68	2.51	C8	50.7	55.4	54.6	53.8
H10ax	3.85	3.97	3.95	4.02	C9	55.2	56.8	55.1	55.1
H10eq	3.63	3.62	3.70	3.58	C10	66.3	68.6	68.2	68.2
H11ax	3.23	3.87	3.80	3.90	C11	69.3	70.1	70.2	70.4
H11eq	3.76	3.92	3.92	3.80	C12	59.8	55.5	53.7	53.5
H12ax	3.58	3.19	3.18	3.25	C13	67.8	69.4	68.8	69.3
H12eq	3.26	2.76	2.54	2.47					
H13ax	3.33	3.41	3.38	3.87					
H13eq	4.09	3.67	3.49	3.53					
NH	11.35	11.24	11.12	10.92					

[a] $^{3}J_{2,3}$ = 8.2 Hz.
[b] $^{3}J_{2,3}$ = 8.0 Hz; $^{3}J_{3,2}$ = $^{3}J_{3,4}$ = 7.7 Hz; $^{4}J_{3,5}$ = 1.0 Hz; $^{4}J_{4,2}$ = 1.1 Hz; $^{3}J_{4,3}$ = $^{3}J_{4,5}$ = 7.6 Hz; $^{3}J_{5,4}$ = 8.1 Hz.
[c] $^{3}J_{2,3}$ = 7.2 Hz; $^{3}J_{5,4}$ = 7.3 Hz.
[d] $^{2}J_{8a,8b}$ = 18.8 Hz; $^{2}J_{9eq,9ax}$ = 12.3 Hz.
[e] $^{3}J_{2,3}$ = 8.1 Hz; $^{3}J_{3,2}$ = $^{3}J_{3,4}$ = 7.5 Hz; $^{3}J_{4,5}$ = $^{3}J_{4,3}$ = 7.8 Hz; $^{3}J_{5,4}$ = 8.1 Hz; $^{2}J_{8a,8b}$ = 16.4 Hz; $^{2}J_{12eq,12ax}$ = 13.7 Hz.
[f] $^{3}J_{2,3}$ = 8.0 Hz; $^{3}J_{3,4}$ = $^{3}J_{3,2}$ = 7.6 Hz; $^{3}J_{4,3}$ = $^{3}J_{4,5}$ = 7.7 Hz; $^{3}J_{5,4}$ = 8.2 Hz; $^{2}J_{8a,8b}$ = 16.1 Hz; $^{2}J_{9eq,9ax}$ = 13.5 Hz; $^{2}J_{10eq,10ax}$ = 10.6 Hz; $^{2}J_{13eq-13ax}$ = 10.6 Hz.
[g] $^{2}J_{8a,8b}$ = 15.8 Hz; $^{2}J_{10eq,10ax}$ = 10.7 Hz; $^{2}J_{13eq,13ax}$ = 10.8 Hz.

The signals due to H8a and H8b protons in $[M(\mathbf{L^2})]^{2+}$ complexes show AB spin patterns where the larger shifts for H8b result from the combined deshielding effects of the benzimidazole ring current and the polarizing effect of the Mn(II) ion on the C-H bond pointing away from it (Fig. 1) [43]. However, a different situation is observed for the complexes of $\mathbf{L^1}$, in which protons H8 are observed as a singlet at room temperature, indicating that the interconversion between the H8a and H8b protons is fast in the NMR scale.

For both the $[M(\mathbf{L^1})]^{2+}$ and $[M(\mathbf{L^2})]^{2+}$ complexes the signal due to the NH protons of benzimidazole groups are progressively shifted to lower fields as the charge density of the metal ion increases from Ba(II) to Mg(II). The ^{1}H NMR chemical shifts observed for the $[Mg(\mathbf{L}^2)]^{2+}$ complexes differ substantially from those observed for the Ca(II) analog, which suggests that these complexes adopt a different structure in solution. This is in line with the structures of these complexes determined in solid state (see below).

Table 5. ^{1}H and ^{13}C NMR spectral data [ppm with respect to TMS] in CD_3CN (298 K) of complexes with $\mathbf{L^3}$ and $\mathbf{L^4}$. See Scheme 1 for labeling.

	Ca[a]	Sr[b]	Ba[c]		Ca	Sr	Ba
$[M(\mathbf{L^3})]^{2+}$							
H2	7.08	7.01	6.97	C1	144.1	144.1	143.9
H3	7.30	7.26	7.26	C2	122.1	121.6	121.2
H4	7.00	6.95	6.93	C3	130.7	130.6	130.7
H5	7.18	7.15	7.14	C4	123.7	123.0	122.5
H7	3.67	3.56	3.52	C5	133.2	133.3	134.0
H8ax	2.71	2.62	2.66	C6	126.9	126.2	125.4
H8eq	2.71	2.69	2.66	C7	60.7	60.0	59.7
H9ax	3.63	3.60	3.61	C8	53.7	52.7	52.6
H9eq	3.45	3.54	3.53	C9	67.6	68.6	68.8
NH_2	4.49	4.31	4.30				
	Ca[d]	Sr[e]			Ca	Sr	
$[M(\mathbf{L^4})]^{2+}$							
H2	6.94	7.06		C1	143.7	144.7	
H3	7.40	7.32		C2	121.2	121.1	
H4	7.08	6.99		C3	131.2	130.9	
H5	7.25	7.19		C4	123.9	123.1	
H7a	3.53	3.58		C5	133.9	133.9	
H7b	3.62	3.58		C6	126.1	125.9	
H8ax	2.81	2.90		C7	56.7	59.5	
H8eq	2.75	2.51		C8	52.2	55.3	
H9ax	4.03	3.89		C9	68.2	69.3	
H9eq	3.74	3.58		C10	70.1	70.5	
H10ax	3.76	3.67		C11	51.8	53.5	
H10eq	3.81	3.67		C12	67.9	69.4	
H11ax	2.63	2.54					
H11eq	2.75	2.87					
H12ax	3.80	3.46					
H12eq	3.65	3.46					
NH_2		4.27					

[a] $^3J_{3,2} = {}^3J_{3,4} = 7.7$ Hz; $^4J_{3,5} = 1.5$ Hz; $^3J_{5,4} = 7.5$ Hz; $^4J_{5,3} = 1.3$ Hz; $^3J_{2,3} = 7.7$ Hz; $^3J_{4,5} = {}^3J_{4,3} = 7.4$ Hz; $^4J_{4,2} = 1.1$ Hz.
[b] $^3J_{3,2} = {}^3J_{3,4} = 7.8$ Hz; $^4J_{3,5} = 1.2$ Hz; $^3J_{5,4} = 7.0$ Hz; $^3J_{2,3} = 7.8$ Hz; $^3J_{4,5} = {}^3J_{4,3} = 7.2$ Hz.
[c] $^3J_{3,2} = {}^3J_{3,4} = 7.8$ Hz; $^4J_{3,5} = 1.3$ Hz; $^3J_{5,4} = 7.5$ Hz; $^4J_{5,3} = 1.3$ Hz; $^3J_{2,3} = 7.9$ Hz; $^3J_{4,5} = {}^3J_{4,3} = 7.4$ Hz.
[d] $^3J_{3,2} = {}^3J_{3,4} = 7.7$ Hz; $^4J_{3,5} = 1.4$ Hz; $^3J_{5,4} = 7.5$ Hz; $^4J_{5,3} = 1.3$ Hz; $^3J_{4,5} = {}^3J_{4,3} = 7.5$ Hz; $^4J_{4,2} = 1.0$ Hz; $^3J_{2,3} = 7.9$ Hz; $^2J_{7a,7b} = 13.3$ Hz.
[e] $^3J_{3,2} = {}^3J_{3,4} = 7.8$ Hz; $^4J_{3,5} = 1.5$ Hz; $^3J_{5,4} = 7.5$ Hz; $^4J_{5,3} = 1.3$ Hz; $^3J_{2,3} = 7.6$ Hz; $^3J_{4,5} = {}^3J_{4,3} = 7.4$ Hz; $^4J_{4,2} = 1.0$ Hz.

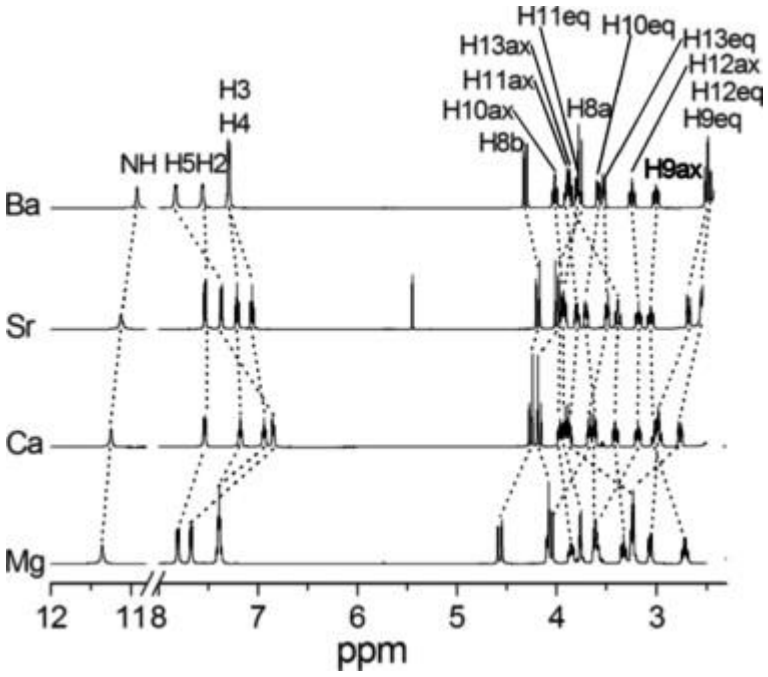

Fig. 1. ^{1}H NMR spectra (500 MHz) of $[M(\mathbf{L^2})]^{2+}$ (M = Mg, Ca, Sr or Ba) complexes recorded in CD_3CN solution at 298 K.

The ^{1}H NMR spectra of the complexes of $\mathbf{L^3}$ and $\mathbf{L^4}$ show essentially the same features than those of the $\mathbf{L^1}$ and $\mathbf{L^2}$ counterparts, but they show broader signals, particularly for $\mathbf{L^3}$ complexes. A similar situation was observed previously when comparing the ^{1}H spectra of the complexes of $\mathbf{L^5}$ and $\mathbf{L^6}$ [24]. This indicates a more important degree of flexibility of the complexes containing aniline pendants in comparison to those with benzimidazole arms. The assignments of the ^{1}H and ^{13}C NMR spectra are summarized in Table 5. The signals observed in the ^{1}H and ^{13}C NMR spectra of the Ca(II) and Sr(II) complexes show very similar chemical shifts, suggesting a similar structure of these complexes in solution.

3.3. Solid state structures

The crystal of compound **1b** contains the $[Mg(\mathbf{L^1})(MeOH)]^{2+}$ or $[Mg(\mathbf{L^1})(H_2O)]^{2+}$ cation, while crystals of compounds **2b**, **3b** and **4b** contain $[Ca(\mathbf{L^1})(MeOH)_2]^{2+}$, $[Sr(\mathbf{L^1})(MeOH)(ClO_4)]^{+}$ and $[Ba(\mathbf{L^1})(MeOH)(ClO_4)_2]$ complex entities, respectively. The perchlorate anions coordinating to Ba(II) in **4b** are involved in hydrogen bonding interaction to the NH groups of benzimidazole units, as previously observed for related systems [44]. Views of the structure of the complexes are shown in Fig. 2, while bond distances of the metal coordination environments are given in Table 6. In all complexes the metal ions are directly bound to the six donor atoms of the ligand. As expected, the coordination number increases upon increasing the ionic radius of the metal ion. The coordination of a methanol molecule (occupation factor 0.819(4)) or a water molecule (occupation factor 0.181(4)) completes seven-coordination around the Mg(II) ion, while the coordination of two methanol molecules results in an eight-coordinate Ca(II) complex. An asymmetrically coordinated bidentate perchlorate anion and a methanol molecule result in the formation of a nine-coordinated Sr(II) complex, and the coordination of two bidentate perchlorate anions gives an 11-coordinate Ba(II) neutral complex [45]. The distances between the metal ions and the tertiary amine nitrogen atoms are considerably longer than those to the nitrogen atoms of the pendant arms. The oxygen atoms of the crown moiety provide the strongest interaction of the ligand to the metal ion, as expected due to the classification the metal ions are hard in the Pearson HSAB [46]. The pendant arms of the ligand are pointing to the same side of the macrocyclic mean plane, resulting a *syn* conformation.

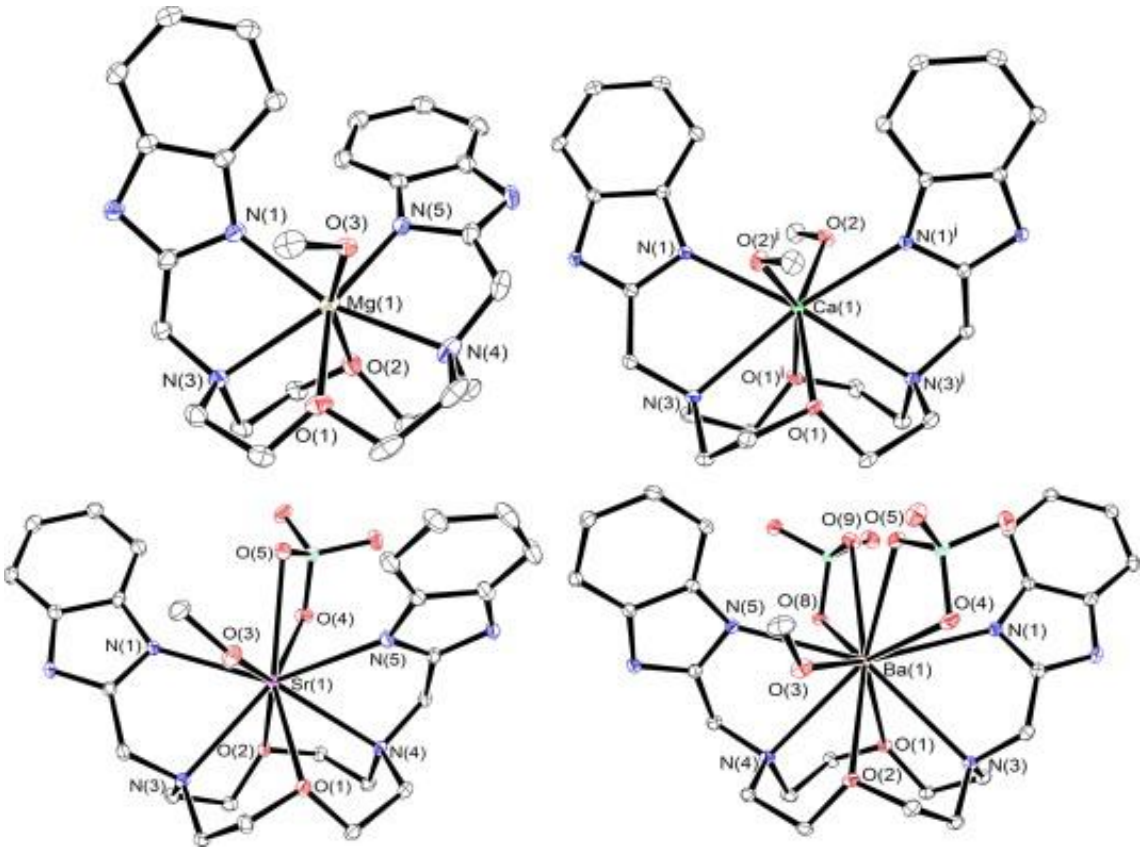

Fig. 2. View of the $[Mg(\mathbf{L^1})(MeOH)]^{2+}$, $[Ca(\mathbf{L^1})(MeOH)_2]^{2+}$, $[Sr(\mathbf{L^1})(MeOH)(ClO_4)]^{+}$ and $[Ba(\mathbf{L^1})(MeOH)(ClO_4)_2]$ entities present in crystals of **1b**, **2b**, **3b** and **4b**, respectively. The ORTEP plots are drawn at the 30% probability level. Hydrogen atoms are omitted for the sake of simplicity.

Table 6. Selected bond lengths (Å) for **1b**, **2b**, **3b** and **4b**.

	1b[a]		**2b**		**3b**		**4b**
Mg(1)–O(3S)	2.115(1)	Ca(1)–O(2)	2.4000(11)	Sr(1)–O(3)	2.500(2)	Ba(1)–O(2)	2.8263(11)
Mg(1)–O(2)	2.168(1)	Ca(1)–O(1)	2.4666(10)	Sr(1)–O(2)	2.6486(19)	Ba(1)–O(3)	2.8269(14)
Mg(1)–N(1)	2.174(2)	Ca(1)–N(1)	2.5122(12)	Sr(1)–O(1)	2.6580(19)	Ba(1)–O(5)	2.8950(12)
Mg(1)–O(1)	2.197(1)	Ca(1)–N(3)	2.7171(12)	Sr(1)–N(5)	2.676(2)	Ba(1)–O(1)	2.9013(11)
Mg(1)–N(5)	2.199(2)			Sr(1)–O(4)	2.681(2)	Ba(1)–N(5)	2.9248(14)
Mg(1)–N(4)	2.322(2)			Sr(1)–N(1)	2.702(2)	Ba(1)–N(1)	2.9381(14)
Mg(1)–N(3)	2.543(2)			Sr(1)–O(5)	2.777(2)	Ba(1)–O(9)	2.9532(12)
				Sr(1)–N(4)	2.806(2)	Ba(1)–N(4)	3.0699(14)
				Sr(1)–N(3)	2.814(2)	Ba(1)–O(8)	3.0772(13)
						Ba(1)–N(3)	3.1293(14)
						Ba(1)–O(4)	3.2086(14)

[a] For compound **1b** the position of the oxygen atom of the water molecule O(3W) and that of the methanol molecule O(3S), affected by substitutional disorder, is exactly the same.

Crystals of **5b** contain the $[Mg(\mathbf{L^2})]^{2+}$ cation and two perchlorate units hydrogen bonded to the NH groups of the pendant arms. The asymmetric unit is comprised of four perchlorate anions and two $[Mg(\mathbf{L^2})]^{2+}$ units with slightly different bond distances and angles. Table 7 summarizes the bond lengths of the metal coordination environment, while the structure of the complex is depicted in Fig. 3. Unlike the Mg(II) complex of $\mathbf{L^1}$, the $[Mg(\mathbf{L^2})]^{2+}$ complex shows a slightly distorted C_2 symmetry, with the receptor $\mathbf{L^2}$ arranged in an *anti* conformation with both pendant arms pointing to opposite sides of the crown moiety. The Mg(II) ion is placed in the macrocyclic cavity with the donor atoms of the pendant arms apically coordinated, which results in a distorted pentagonal bipyramidal coordination environment around the metal ion. The equatorial plane of the pentagonal bipyramid is defined by the three ether oxygen atoms and the two pivotal nitrogen atoms (mean deviation from planarity 0.150 Å). The polyhedron is axially compressed, since the apical bonds are significantly shorter than equatorial bonds. Angle N(1)–Mg(1)–N(5) [170.47(16)°] deviates by ca. 9.5° from the ideal value for a regular pentagonal bipyramid (180°). Angles D(1)–Mg(1)–D(2), where D(1) and D(2) represent adjacent donor atoms of the equatorial plane, are also close to the ideal value of 72° (70.0–78.3°) and the vectors defined by the metal ion and the axial donors N(1) and N(5) form angles that are relatively close to 90° with the vectors containing the metal ion and the equatorial donor atoms (85.4–94.9°), as expected for a pentagonal bipyramidal coordination environment. The overall structure of the complex is similar to that reported previously for the Zn(II) analog [43].

Table 7. Selected bond lengths (Å) for **5b**, **6b**, **7b** and **8**.

	5b		**6b**		**7b**		**8**
Mg(1)–N(1)	2.153(4)	Ca(1)–O(4)	2.399(2)	Sr(1)–O(2)	2.595(3)	Ba(1)–O(2)	2.805(2)
Mg(1)–N(5)	2.163(4)	Ca(1)–O(3)	2.429(2)	Sr(1)–O(3)	2.598(3)	Ba(1)–O(4)	2.808(2)
Mg(1)–O(3)	2.178(4)	Ca(1)–O(2)	2.462(2)	Sr(1)–O(4)	2.648(3)	Ba(1)–O(3)	2.820(2)
Mg(1)–O(1)	2.191(4)	Ca(1)–N(5)	2.496(2)	Sr(1)–N(1)	2.675(3)	Ba(1)–O(1)	2.849(2)
Mg(1)–O(2)	2.204(4)	Ca(1)–O(1)	2.535(2)	Sr(1)–N(5)	2.683(3)	Ba(1)–N(5)	2.867(3)
Mg(1)–N(3)	2.311(4)	Ca(1)–N(1)	2.545(2)	Sr(1)–O(1)	2.691(3)	Ba(1)–O(8)	2.913(2)
Mg(1)–N(4)	2.314(4)	Ca(1)–N(3)	2.662(2)	Sr(1)–N(3)	2.777(3)	Ba(1)–O(9)	2.915(2)
Mg(2)–N(7)	2.147(5)	Ca(1)–N(4)	2.724(2)	Sr(1)–O(5)	2.821(3)	Ba(1)–N(1)	2.933(3)
Mg(2)–N(11)	2.148(5)			Sr(1)–N(4)	2.838(3)	Ba(1)–N(4)	2.946(3)
Mg(2)–O(4)	2.182(4)					Ba(1)–N(3)	2.963(3)
Mg(2)–O(5)	2.185(4)						
Mg(2)–O(6)	2.218(4)						
Mg(2)–N(10)	2.297(5)						
Mg(2)–N(9)	2.320(5)						

[a] For compound **1b** the position of the oxygen atom of the water molecule O(3W) and that of the methanol molecule O(3S), affected by substitutional disorder, is exactly the same.

Crystals of **6b** and **7b** contain the $[M(\mathbf{L^2})(ClO_4)]^+$ cations (M = Ca or Sr) and a perchlorate anion hydrogen-bonded to the NH groups of benzimidazole pendant arms. In the case of **7b** acetonitrile and ethanol molecules are also present in the crystal lattice, the latter participating in a hydrogen-bonding interaction with the NH groups of benzimidazole units. The receptor adopts a *syn* conformation, with the metal ion being directly bonded to its seven donor atoms and an oxygen atom of a monodentate [Ca(II)] or bidentate [Sr(II)] perchlorate ligand. Crystals of **8** contain the $[Ba(\mathbf{L^2})(ClO_4)_2]$ unit with the receptor again adopting a *syn* conformation. One of the perchlorate groups coordinates in a bidentate fashion, while the second one is

monodentated, which results in 10-coordination around the Ba(II) ion. Views of the structures of the $[M(\mathbf{L^2})(ClO_4)]^+$ (M = Ca or Sr) and $[Ba(\mathbf{L^2})(ClO_4)_2]$ units are shown in Fig. 3, while bond distances of the metal coordination environments are summarized in Table 7.

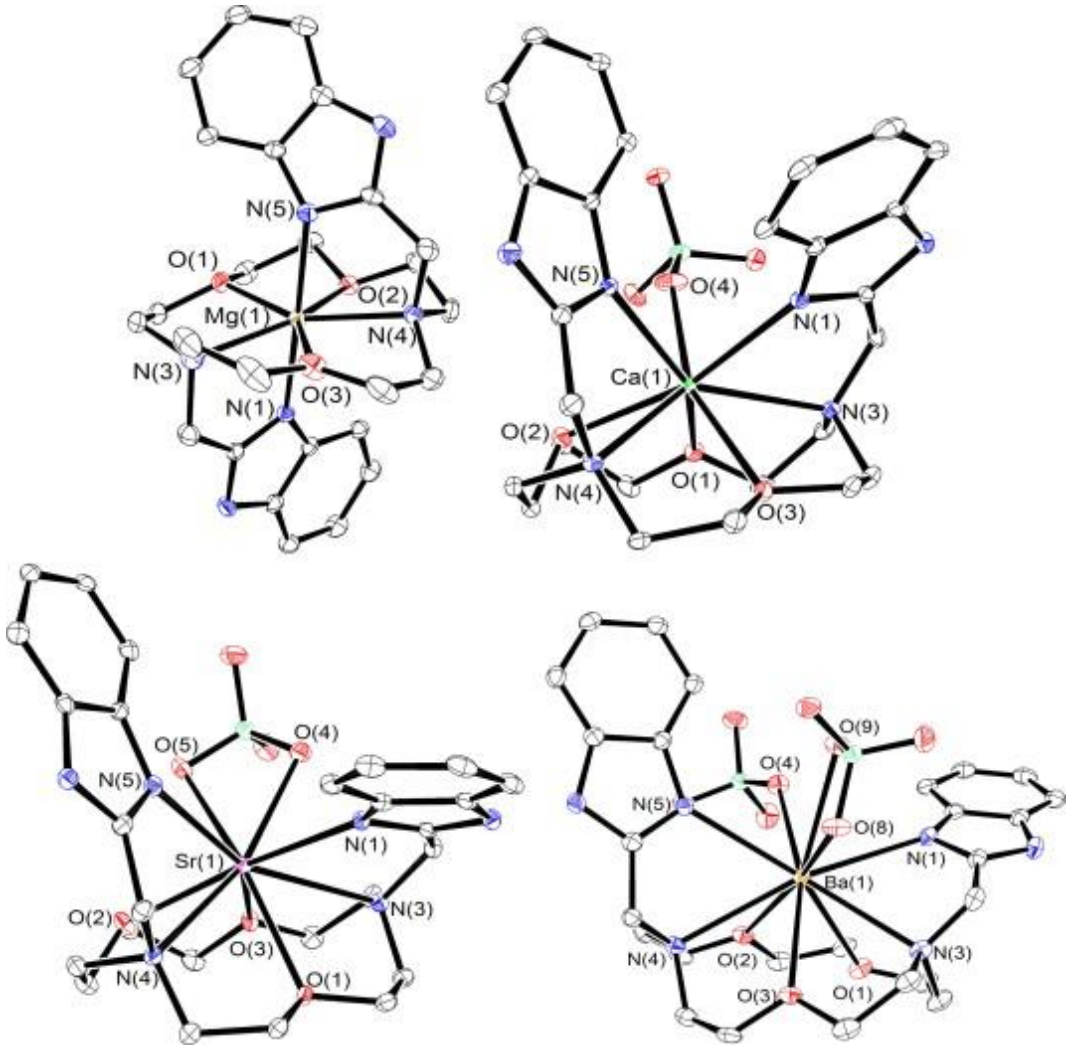

Fig. 3. View of the $[Mg(\mathbf{L^2})]^{2+}$, $[Ca(\mathbf{L^2})(ClO_4)]^+$, $[Sr(\mathbf{L^2})(ClO_4)]^+$ and $[Ba(\mathbf{L^2})(ClO_4)_2]$ units present in crystals of **5b**, **6b**, **7b** and **8**. The ORTEP plots are drawn at the 30% probability level. Hydrogen atoms are omitted for the sake of simplicity.

The structure of the uncoordinated receptor $\mathbf{L^3}$ was determined by X-ray diffraction analysis. The arms of the lariat ether are arranged on opposite sides of the crown moiety, resulting in an *anti* conformation. The conformation of the receptor is conditioned by hydrogen-bonding interactions between the NH_2 groups of aniline units and the nitrogen atoms of the crown moiety [N1-H1N 0.87(2) Å, N2···H1N 2.42(2) Å, N1···N2 3.053(2), N1–H1N···N2 130(1)°]. The X-ray crystal structure of its Ca(II) complex (**9b**) allows us to see the dramatic change on the receptor conformation as, as shown in Fig. 4. The receptor adopts a *syn* conformation in the complexes, in contrast to the situation observed for the uncoordinated receptor $\mathbf{L^3}$. Crystals of compound **9b** show a substitutional disorder, as one coordination position is occupied alternatively by a water molecule (occupation factor 0.66(2)) or by an ethanol molecule (occupation factor 0.34(2)). However, the coordination environment of the Ca(II) ion in $[Ca(\mathbf{L^3})(H_2O)_2]^{2+}$ and $[Ca(\mathbf{L^3})(H_2O)(EtOH)]^{2+}$ is exactly the same because the oxygen atom of water or ethanol is exactly in the same position. The non-coordinated perchlorate anions are involved in intermolecular hydrogen-bonding interaction with the -NH_2 groups of the

ligand. Bond distances and angles of the metal coordination environment are given in Table 8. A quite similar situation is found in crystals of **13** containing the $[Sr(\mathbf{L^4})(ClO_4)]^+$ cation (Fig. 4) and a non-coordinated perchlorate anion; although in this case the coordinated perchlorate anion is also involved in intramolecular hydrogen bonding interaction with one of the $–NH_2$ groups of the ligand [N1-H22N 0.85(3) Å, O11···H22N 2.32(3) Å, N1···O11 3.087(3), N1–H22N···O11 149(2)°] (see Fig. 4). In both cases, the distances between the metal ions and the donor atoms of the pendant arms [N(1) and N(4)] are comparable to those to the nitrogen atoms of the macrocycle, while the oxygen atoms of the crown moiety provide the strongest interaction of the ligand to the metal ion.

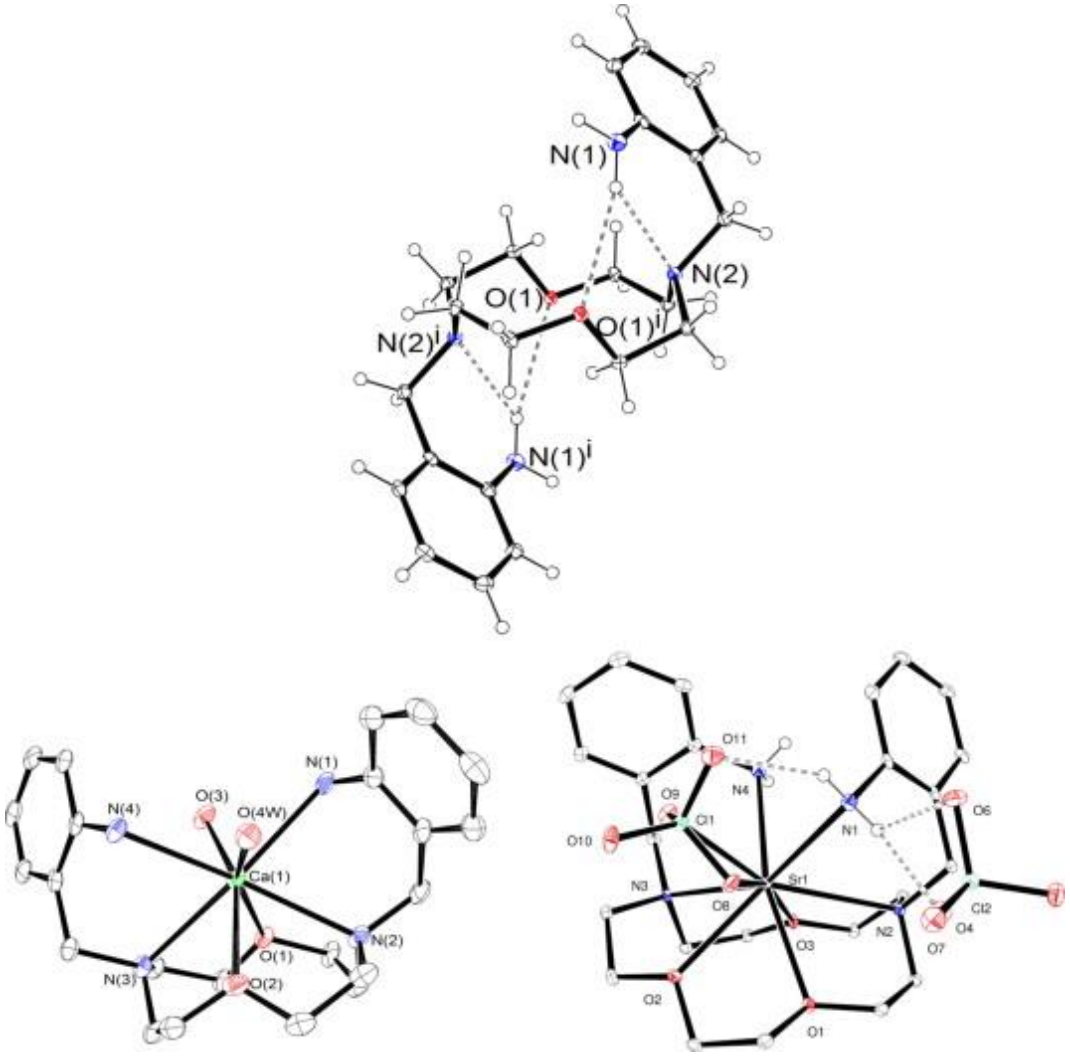

Fig. 4. View of the $\mathbf{L^3}$, $[Ca(\mathbf{L^3})(H_2O)_2]^{2+}$ and $[Sr(\mathbf{L^4})(ClO_4)](ClO_4)$ units present in crystals of $\mathbf{L^3}$, **9b** and **13**. The ORTEP plots are drawn at the 30% probability level. The view of the $[Sr(\mathbf{L^4})(ClO_4)](ClO_4)$ entity present in **13** shows the intramolecular hydrogen bonding interactions involving both coordinated and non-coordinated perchlorate anions and $–NH_2$ groups.

A comparison of the X-ray structures reported in this work shows that the coordination number increases gradually upon increasing the radius of the metal ion, the Mg(II), Ca(II), Sr(II) and Ba(II) complexes showing coordination numbers 7, 8, 9 and 10, respectively. The receptors coordinate to the respective metal ion through all available donor atoms, the coordination requirements of each metal ion being satisfied by the presence of additional ligands such as water, methanol or perchlorate anions. In addition, perchlorate anions can act as monodentate or bidentate ligands depending on the metal ion size. The distances between the

metal ions and the donor atoms of the crown moiety are similar to those observed for eight-coordinate Ca(II) [47-50], nine-coordinate Sr(II) [51] and 10-coordinate Ba(II) [23,52,53] complexes with ligands containing diaza crown ethers. An *anti* conformation of the ligand is only observed for the $[Mg(\mathbf{L^2})]^{2+}$ complex, most likely due to the small ionic radius of Mg(II) and the relatively large size of the crown moiety fragment. For the remaining complexes investigated by X-ray crystallography the metal ion is too large to fit inside the macrocyclic cavity, which favors a *syn* conformation. This in contrast with structures observed in the solid state for the Ca(II) and Sr(II) complexes of $\mathbf{L^6}$, which present an *anti* conformation of the ligand. Both the complexes of $\mathbf{L^5}$ and $\mathbf{L^6}$ exist in acetonitrile solution as a mixture of *syn* and *anti* conformers [24].

Table 8. Selected bond lengths (Å) for **9b** and **13**.

	9b[a]		**13**
Ca(1)–O(2)	2.403(3)	Sr(1)–O(3)	2.5826(15)
Ca(1)–O(4W)[a]	2.424(4)	Sr(1)–O(1)	2.5978(15)
Ca(1)–O(3)	2.434(4)	Sr(1)–O(2)	2.6030(15)
Ca(1)–O(1)	2.438(3)	Sr(1)–O(9)	2.6683(16)
Ca(1)–N(4)	2.591(4)	Sr(1)–N(4)	2.727(2)
Ca(1)–N(1)	2.606(4)	Sr(1)–N(3)	2.7416(19)
Ca(1)–N(2)	2.662(4)	Sr(1)–N(1)	2.791(2)
Ca(1)–N(3)	2.699(4)	Sr(1)–N(2)	2.8137(18)
		Sr(1)–O(8)	2.8980(17)

[a] For compound **9b** the position of the oxygen of the water molecule O(4W) and that of the ethanol molecule(O4S), affected by substitutional disorder, is exactly the same.

Table 9. Distance between the metal ion and the centroid defined by the donor atoms of the macrocyclic fragment (Å), distance between the amine nitrogen atoms of the macrocycle (Å) and angle defined by the nitrogen atoms of the macrocycle and the metal ion (°) for the complexes reported in this work.

	M(II)–centroid	N_{AM}–M(II)–N_{AM}	$N_{AM}\cdots N_{AM}$
$[Mg(\mathbf{L^1})(H_2O)]^{2+}$	1.28	126.4	4.34
$[Ca(\mathbf{L^1})(MeOH)_2]^{2+}$	1.64	107.60	4.39
$[Sr(\mathbf{L^1})(MeOH)(ClO_4)]^{+}$	1.83	100.78	4.33
$[Ba(\mathbf{L^1})(MeOH)(ClO_4)_2]$	2.18	91.46	4.44
$[Mg(\mathbf{L^2})]^{2+}$	0.00	140.19	4.35
$[Ca(\mathbf{L^2})(ClO_4)]^{+}$	1.09	134.20	4.96
$[Sr(\mathbf{L^2})(ClO_4)]^{+}$	1.35	125.23	4.99
$[Ba(\mathbf{L^2})(ClO_4)_2]$	1.69	116.16	5.02
$\mathbf{L^2}$			4.49
$[Ca(\mathbf{L^3})(H_2O)]^{2+}$	1.58	111.95	4.44
$[Sr(\mathbf{L^4})(ClO_4)]^{+}$	1.36	125.53	4.94

For the complexes of $\mathbf{L^1}$, the distances between the metal ions and the centroids defined by the donor atoms of the crown moiety (M(II)–centroid, Table 9) increase upon increasing the ionic radius of the metal ion. As

a result, the angles defined by the amine nitrogen atoms of the macrocycle and the metal ion decrease from Mg(II) to Ba(II) as the metal ion size increases. However, the distances between the amine nitrogen atoms of the macrocyclic unit ($N_{AM}\cdots N_{AM}$) appear to be relatively insensitive to the size of the metal ion as a consequence of the important degree of rigidity of the 1,7-diaza-12-crown-4 moiety. As a consequence, the $N_{AM}\cdots N_{AM}$ distance observed for the Ca(II) complex of **L**^{3} is similar to those observed for the complexes of **L**^{1}, and also to that found in the free ligand **L**^{3}. For the complexes of **L**^{2} the distance between amine nitrogen atoms increases substantially from Mg(II) (4.35 Å) to Ca(II) (4.96 Å), which shows that the relatively large crown unit of **L**^{2} allows the ligand to change its conformation to accommodate metal ions of different size.

4. Conclusions

Herein we have reported a detailed analysis of the solid state structures of a series of complexes of group 2 metal ions with lariat ethers derived from 1,7-diaza-15-crown-5 or 1,7-diaza-12-crown-4. The structures determined by X-ray diffraction analysis show hexadentate binding of **L**^{1} and **L**^{3}, and heptadentate binding of **L**^{2} and **L**^{4} to all metal ions investigated, which is compatible with the ^{1}H and ^{13}C NMR spectra of the complexes in CD_3CN solution. In the solid state the coordination number increases from seven for Mg(II) complexes to 10 or 11 for the Ba(II) analogs through the coordination of solvent molecules (methanol or water) or perchlorate anions.

Acknowledgements

The authors thank Xunta de Galicia (IN845B-2010/063) for generous financial support. I.C.-B, A.R.-R. and M.R.-F. thank the Spanish Ministerio de Educación y Ciencia (FPU program) for predoctoral fellowships.

Supplementary data

CCDC 825765, 825766, 825767, 825768, 825769, 825770, 825771, 825772, 825773, 825774 and 825775 contain the supplementary crystallographic data for compounds **13**, **1b**, **2b**, **3b**¸**4b**, **5b**, **6b**, **7b**, **8**, **9b** and **L**^{3}, respectively. These data can be obtained free of charge via http://www.ccdc.cam.ac.uk/conts/retrieving.html, or from the Cambridge Crystallographic Data Centre, 12 Union Road, Cambridge CB2 1EZ, UK; fax: (+44) 1223-336-033; or e-mail: deposit@ccdc.cam.ac.uk.

References

[1] C.J. Pederson, J.-M. Lehn, D.J. Cram, Resonance 6 (2001) 71.

[2] G.W. Gokel, S.H. Korzeniowski, Macrocyclic Polyether Synthesis, Springer, Berlin, 1982.

[3] G.W. Gokel, O.F. Schall, in: G.W. Gokel (Ed.), Comprehensive Supramolecular Chemistry, Lariat Ethers, vol. 1, Elsevier, Oxford, 1996, pp. 97–152.

[4] G.W. Gokel, W.M. Leevy, M.E. Weber, Chem. Rev. 248 (2004) 2723.

[5] H.-J. Schneider, A.K. Yatsimirsky, Chem. Soc. Rev. 37 (2008) 263.

[6] X.-J. Ju, S.-B. Zhang, M.-Y. Zhou, R. Xie, L. Yang, L.-Y. Chu, J. Hazard. Mater. 167 (2009) 114.

[7] V.K. Gupta, M.K. Pal, A.K. Singh, Anal. Chim. Acta 631 (2009) 161.

[8] P. Buhlmann, E. Pretsch, E. Bakker, Chem. Rev. 98 (1998) 1593.

[9] M.H. Hyun, J. Sep. Sci. 26 (2003) 242.

[10] A.V. Tsukanov, A.D. Dubonosov, V.A. Bren, V.I. Minkin, Chem. Hetercycle Comp. 44 (2008) 899.

[11] I. Moczar, P. Huszthy, A. Mezei, M. Kadar, J. Nyitrai, K. Toth, Tetrahedron 66 (2010) 350.

[12] V.I. Minkin, A.D. Dubonosov, V.A. Bren, A.V. Tsukanov, ARKIVOK (2008) 90.

[13] N. Basilio, L. Garcia-Rio, J.C. Mejuto, M. Perez-Lorenzo, J. Org. Chem. 71 (2006) 4280.

[14] S. Shirakawa, K. Yamamoto, M. Kitamura, T. Ooi, K. Maruoka, Angew. Chem., Int. Ed. 44 (2005) 625.

[15] A. Casnati, A. Pochini, R. Húngaro, C. Bocchi, F. Ugozzoli, R.J.M. Egberink, H. Struijk, R. Lugtenberg, F. de Jong, D.N. Reinhoudt, Chem. Eur. J. 2 (1996) 436.

[16] K. Marijeta, L. Tusek-Bozic, L. Frkanec, ChemMedChem 3 (2008) 1478.

[17] T. Wiegand, J. Karr, J. Steinkruger, K. Hiebner, B. Simetich, M. Beatty, J. Redepenning, Chem. Mater. 20 (2008) 5016.

[18] W. Catterall, A. Few, Neuron Rev. 59 (2008) 882.

[19] A. Hartwig, Mutat. Res. 475 (2001) 113.

[20] P.J. Marie, P. Ammann, G. Boivin, C. Rey, Calcif. Tissue Int. 69 (2001) 121.

[21] S.C. Verberckmoes, M.E. De Broe, P.C. D'Haese, Kidney Int. 64 (2003) 534.

[22] K. Usuda, K. Kono, T. Dote, M. Watanabe, H. Shimizu, Y. Tanimoto, E. Yamadori, Environ. Health Prev. Med. 12 (2007) 231.

[23] C. Platas-Iglesias, D. Esteban, V. Ojea, F. Avecilla, A. de Blas, T. Rodríguez-Blas, Inorg. Chem. 42 (2003) 4299.

[24] I. Carreira-Barral, A. Rodríguez-Rodríguez, M. Regueiro-Figueroa, D. Esteban-Gómez, C. Platas-Iglesias, A. de Blas, T. Rodríguez-Blas, Inorg. Chim. Acta 370 (2011) 270.

[25] M. Regueiro-Figueroa, D. Esteban-Gómez, C. Platas-Iglesias, A. de Blas, T. Rodríguez-Blas, Eur. J. Inorg. Chem. (2007) 2198.

[26] M. Gonzalez-Lorenzo, C. Platas-Iglesias, F. Avecilla, S. Faulkner, S.J.A. Pope, A. de Blas, T. Rodríguez-Blas, Inorg. Chem. 44 (2005) 4254.

[27] C. Rodríguez-Infante, D. Esteban, F. Avecilla, A. de Blas, T. Rodríguez-Blas, J. Mahia, A.L. Macedo, C.F.G.C. Geraldes, Inorg. Chim. Acta 317 (2001) 190.

[28] W.C. Wolsey, J. Chem. Educ. 50 (1973) A335.

[29] SADABS Version 2008/1, Sheldrick, Bruker AXS Inc.

[30] WinGX 1.70.01, An Integrated System of Windows Programs for the Solution, Refinement and Analysis of Single Crystal X-ray Diffraction Data L.J. Farrugia, J. Appl. Crystallogr. 32 (1999) 837.

[31] DIRDIF2008 P.T. Beurskens, G. Beurskens, R. de Gelder, S. Garcia-Granda, R.O. Gould, J.M.M. Smits, The DIRDIF2008 Program System, Crystallography Laboratory, University of Nijmegen, The Netherlands, 2008.

[32] SIR92 A. Altomare, G. Cascarano, C. Giacovazzo, A. Guagliardi, J. Appl. Crystallogr. 26 (1993) 343.

[33] G.M. Sheldrick, Acta Crystallogr. A64 (2008) 112.

[34] Superflip – A Computer Program for the Solution of Crystal Structures by Charge Flipping in Arbitrary Dimensions L. Palatinus, G. Chapuis, J. Appl. Crystallogr. 40 (2007) 786.

[35] M. Nardelli, J. Appl. Crystallogr. 32 (1999) 563.

[36] D. Esteban, D. Bañobre, R. Bastida, A. de Blas, A. Macías, A. Rodríguez, T. Rodríguez-Blas, D.E. Fenton, H. Adams, J. Mahía, Inorg. Chem. 38 (1999) 1937.

[37] K. Nakamoto, Infrared and Raman Spectra of Inorganic and Coordination Compounds, third ed., John Wiley, New York, Chichester, Brisbane, Toronto, 1972. pp. 142–154.

[38] W.J. Geary, Coord. Chem. Rev. 7 (1971) 81.

[39] J.K. Beattie, Acc. Chem. Res. 4 (1971) 253.

[40] S. Aime, M. Botta, G. Ermondi, Inorg. Chem. 31 (1992) 4291.

[41] M. Karplus, J. Am. Chem. Soc. 85 (1963) 2870.

[42] C.F.G.C. Geraldes, A.D. Sherry, G.E. Kiefer, J. Magn. Reson. 97 (1992) 290.

[43] L. Vaiana, M. Regueiro-Figueroa, M. Mato-Iglesias, C. Platas-Iglesias, D. Esteban-Gómez, A. de Blas, T. Rodríguez-Blas, Inorg. Chem. 46 (2007) 8271.

[44] L. Vaiana, D. Esteban-Gómez, M. Mato-Iglesias, C. Platas-Iglesias, A. de Blas, T. Rodríguez-Blas, Eur. J. Inorg. Chem. (2009) 400.

[45] P.K. Sazonov, L.K. Minacheva, A.V. Churakov, V.S. Sergienko, G.A. Artamkina, Y.F. Oprunenko, I.P. Beletskaya, Dalton Trans. (2009) 843.

[46] R.G. Pearson, R.J. Mawby, Halogen Chem. 3 (1967) 55.

[47] M.B. Duriska, S.M. Neville, S.R. Batten, Chem. Commun. (2009) 5579.

[48] R. Ferreirós-Martínez, D. Esteban-Gómez, A. de Blas, C. Platas-Iglesias, T. Rodríguez-Blas, Inorg. Chem. 48 (2009) 11821.

[49] J. Hu, L.J. Barbour, R. Ferdani, G.W. Gokel, J. Supramol. Chem. 1 (2001) 157.

[50] J. Hu, L.J. Barbour, R. Ferdani, G.W. Gokel, Chem. Commun. (2002) 1806.

[51] A.S. De Sousa, R.D. Hancock, J.H. Reibenspies, J. Chem. Soc., Dalton Trans. (1997) 939.

[52] F. Avecilla, D. Esteban, C. Platas-Iglesias, A. de Blas, T. Rodríguez-Blas, Acta Crystallogr. C59 (2003) m16.

[53] S.H. Chan, W.T. Wong, W.K. Chan, Chem. Mater. 13 (2001) 4635.